



Los Alamos

NATIONAL LABORATORY

memorandum

LANSCE Division

To/MS: Distribution

From/MS: James H. Billen/H817

Phone/FAX: 7-6627/5-2904

Email: JBillen@lanl.gov

Symbol: LANSCE-1:99-142

Date: July 27, 1999

SUBJECT: Coupled-Cavity Drift-Tube Linac Design for SNS

This memo reports the redesign of the coupled-cavity drift-tube linac (CCDTL) for use in the low-energy part of the SNS linac. The cavity shapes described here replace the ones reported in memorandum AOT-1:TNM97-049, "Representative CCDTL Cavities for the National Spallation Neutron Source," dated February 28, 1997. We have used the earlier design for beam dynamics design studies for the past several years. The main difference between the old and new designs is the addition of a tuning ring on the cavity equator. This ring allows a design that satisfies space requirements between cavity segments.

Requirements

The first requirement, which was the reason for the redesign, is that the outer cavity diameter must be large enough to provide sufficient radial space for quadrupole magnets under the intersegment coupling cavities. A desirable feature, which the new design can accommodate, is a constant value for the cavity diameter over the entire length of the CCDTL. In the previous design, the final cavity diameter (after adjustment to compensate for the frequency effects of stems and coupling slots) ranged from 23.7 cm (at $\beta = 0.20$) to 20.6 cm (at $\beta = 0.39$). Nathan Bultman has requested that the cavity diameter exceed 22.5 cm.

At the time of this writing, the beam-dynamics design uses the CCDTL structure between beam energies of 20 and about 80 MeV, which correspond to H^- particle velocities between $\beta = 0.20$ and $\beta = 0.39$. Error studies have indicated the need for a larger bore radius R_b than initially assumed for this structure. Earlier designs had $R_b = 1.00$ to 1.25 cm. However, the poor beam quality after passing through the medium-energy beam transport (MEBT) has forced us to increase the radius to $R_b = 1.5$ cm to reduce beam loss. This increase in bore radius has decreased considerably the maximum achievable shunt impedance.

The present beam-dynamics design provides guidance on required field level E_0T , where E_0 is the average axial electric field and T is the transit-time factor. The lowest E_0T (~ 1.92 MV/m) occurs at the low-energy end and the highest field (~ 3.09 MV/m) occurs at the high-energy end. To prevent sparking at regions of high surface electric field, we adjust the nose shape and gap length so that the surface electric fields do not exceed 1.5 times the Kilpatrick field, or 1.5×26.06 MV/m = 39.09 MV/m at 805 MHz.

Each segment of CCDTL structure (between pairs of quadrupole magnets) consists of two identical cavities, each cavity containing one drift tube and two accelerating gaps. Successive segments increase in length as the particle velocity increases. To evaluate cavity efficiency and power losses, we assume 5% coupling between cavities. During preparation of the Conceptual Design Report we chose 5% coupling for the entire linac because it provided tolerable power-flow field droop and negligible power-flow phase shifts in the rf modules.

Cavity Design Features

We use the program CDTFISH in the Poisson Superfish code distribution to design the cavity shape and compute surface fields and rf power losses. Figure 1 shows the basic outline of CCDTL cavity generated by CDTFISH. The details near the wall nose are shown in Figure 2 and the details of the drift-tube nose are in Figure 3. An optional tuning ring on the cavity equator (not shown in Figure 1) appears in Figure 4. The lower edge of these figures of revolution is the center of the bore tube of radius R_b . The cavity diameter is D and s is the septum thickness between cavities. The inner-nose radius R_i (R_{di} on internal drift tubes) connects the bore tube to an optional vertical flat segment of length F (or F_d). The outer-nose radius R_o (R_{do} on internal drift tubes) connects the flat segment on the nose with the cone angle segment. The two nose arcs are tangent if $F = 0$ (or $F_d = 0$). The face angle α_f in Figure 3 is the angle that the drift-tube face makes with the vertical. The cone angle α_c in Figure 2 is the angle that the nose makes with the horizontal.

The cavity wall has an outer corner radius R_{co} and an inner corner radius R_{ci} . The bore-tube extension δT_R on the right-hand side of the cavity models the end cavity of a structure consisting of two or more one-drift-tube cavities between drift spaces. For the SNS design there are two cavities per segment. The full length of the problem geometry is $L + \delta T_L + \delta T_R$, where L is defined in terms of the number of gaps N_g and $\beta\lambda$. (In Figure 1 $\delta T_L = 0$.) The code uses a Dirichlet boundary condition on the left edge of the bore hole. On the right side, the bore tube is long enough so the fields fall to negligible values at the edge of the geometry. Neither Dirichlet nor Neumann boundaries would be appropriate at this edge.

Both gaps in a cavity have the same length g . The CDTFISH code automatically adjusts the gap centers and reports the shifts (δg_1 and δg_2) that properly locate the electrical centers of each cell. As shown in Figure 1, δg_1 refers to a gap on the side of the CCDTL cavity adjacent to another cavity; and δg_2 refers to a gap at the very end of a segment where the fields can penetrate into the connecting bore tube between segments. The gap center always shifts towards the outside of the cavity, that is, in such a way as to lengthen the internal drift tube. Larger bore radii result in larger shifts.

Figure 4 defines the geometrical parameters for a tuning ring in the CCDTL cavity. The CDTFISH code includes the ring if the user supplies nonzero values for both the ring width W_{Ring} and depth D_{Ring} . The inner and outer (with respect to the location in the cavity) radii $R_{Ring,i}$ and $R_{Ring,o}$ are optional. For SNS cavities $R_{Ring,i} = R_{Ring,o} = 0.25$ cm. The sum of the two ring radii may

be larger or smaller than the ring depth. If the radii are small, the code will connect the two arcs with a vertical line segment. If the radii are large (as shown in Figure 4), the arcs meet tangent to one another.

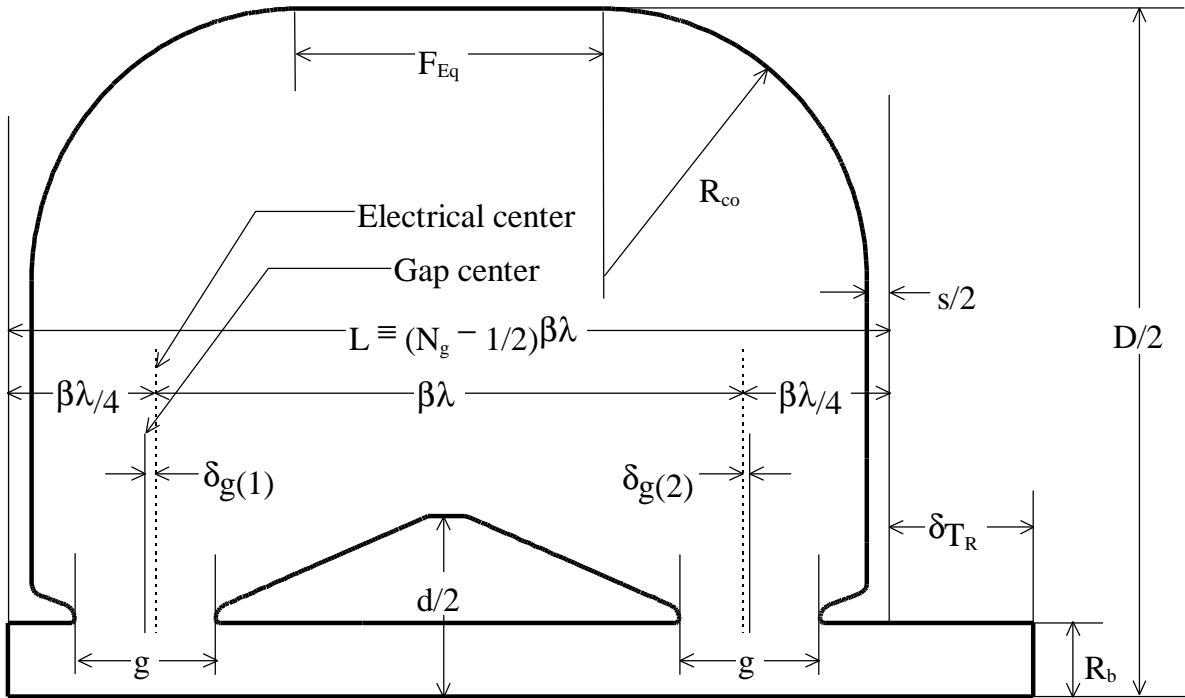


Figure 1. A one-drift-tube, 2-gap CCDTL cavity. The nominal cavity length L is a half integral multiple of the length bl ($3bl/2$ in this case). The full geometry is longer by an amount equal to the bore-tube extension. Both drift-tube gaps are exactly the same length. The code moves the gap centers to make the cell's electrical centers bl apart and $bl/4$ from the nominal edges of the cavity.

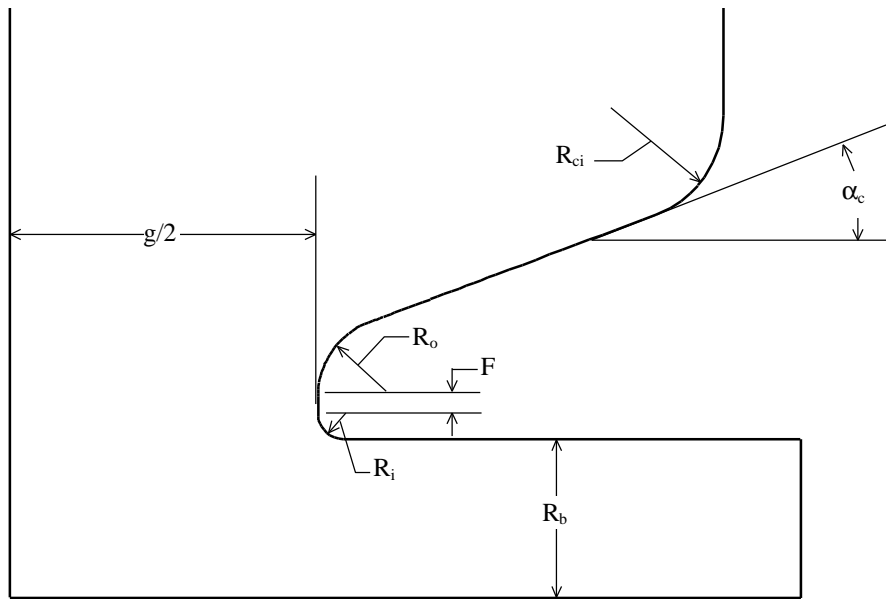


Figure 2. Detail of a nose on the cavity wall in the CCDTL cavity. By convention, the cone angle measured from horizontal defines the sloped segment on the cavity-wall nose.

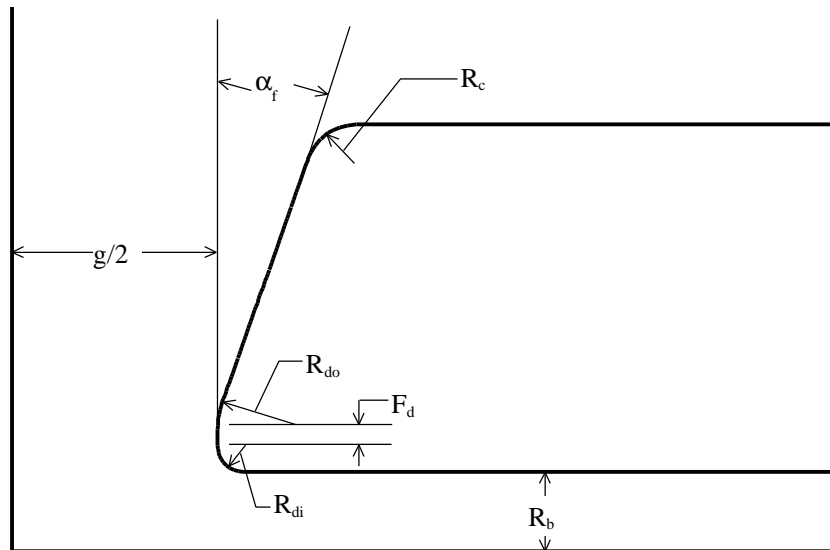


Figure 3. Detail near the drift-tube nose. By convention, the face angle measured from the vertical defines the slope on internal drift tubes.

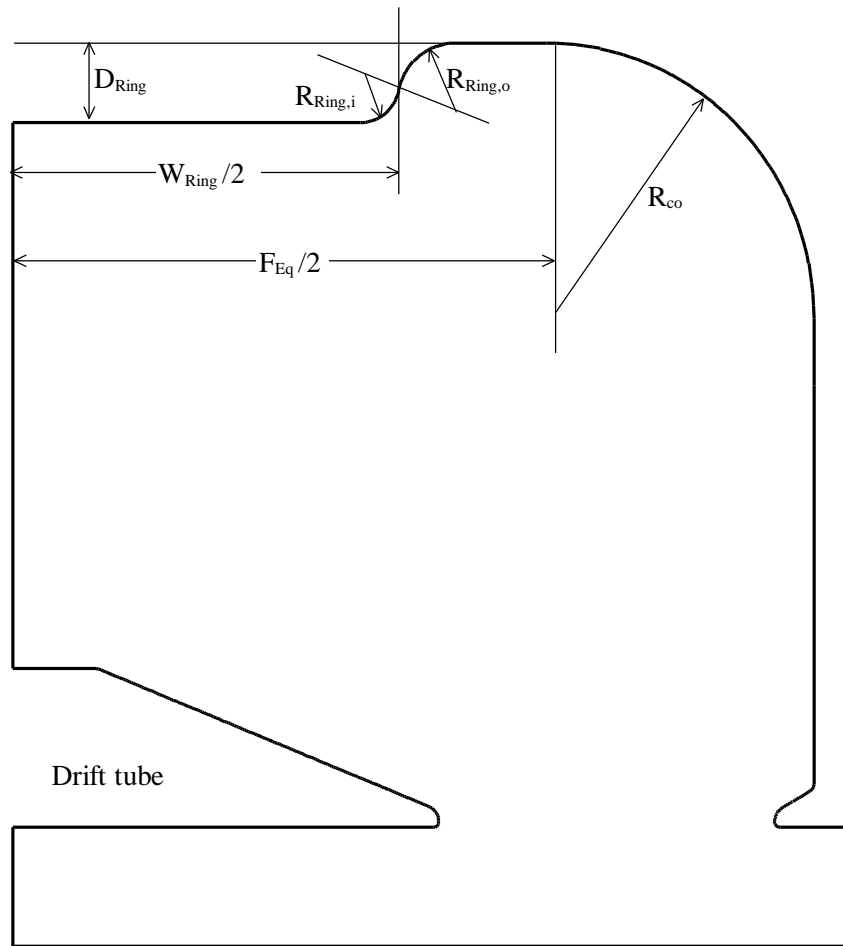


Figure 4. Details of the tuning ring in a CCDTL cavity. The ring, including its outer radius, fits entirely within the equator flat. The two ring radii are optional and their sum may be larger or smaller than the ring depth.

Design Parameters for SNS

Figure 5 shows the cavity shapes at both ends of the CCDTL velocity range in the SNS linac. The cavity shapes have been optimized for high shunt impedance subject to two main constraints that apply over the entire velocity range: 1) the cavity diameter has the fixed value $D = 22.75$ cm, and 2) the peak surface electric does not exceed ~ 1.45 Kilpatrick at the operating field levels used in the current beam-dynamics design. The 22.75-cm cavity diameter provides the radial space under

the coupling cavities requested by SNS mechanical engineers. One of our original goals in the cavity design was to keep the surface field below 1.5 Kilpatrick. In previous efforts to reduce the number of rf modules, some beam-dynamics design iterations have exceeded this limit at the high-energy end of the CCDTL. Therefore, in the redesign we have imposed the limit of 1.45 Kilpatrick at the current design fields in order to provide a few percent margin for any future rf partitioning of the linac.

Optimizing the shunt impedance involved varying the nose radii on internal drift tubes (R_{di} and R_{do}) and on the outer wall (R_i and R_o), the drift-tube face angle α_f , the drift-tube diameter d , the outer corner radius R_{co} , and the inner corner radius R_{ci} . The two sets of nose radii vary together, keeping the ratios constant: $R_o/R_i = R_{do}/R_{di} = 3$. Previous work has shown that the ratio of ~ 3 is optimum for low peak surface electric field at a given gap length. For each choice of different geometrical parameters, the CDTFISH code adjusted the gap length g for resonance at 805 MHz. (The code simultaneously adjusts the gap centers to properly locate the electrical center of each gap.) The results of the optimization study showed that we can fix many of the cavity parameters over the entire velocity range of the CCDTL. Table 1 lists the parameters of the CCDTL that are the same in all cavities, and Table 2 lists geometric parameters that vary with particle velocity. All the data in Table 2 are in cm (except columns 1 and 3, which are dimensionless).

Table 1. CCDTL Fixed Parameters.

Parameter	Symbol	Value
Resonant frequency	f	805 MHz
Operating temperature	T_{op}	90 F
Cavity diameter	D	22.75 cm
Bore radius	R_b	1.50 cm
Cone angle	α_c	30 degrees
Inner nose radius	R_i	0.07 cm
Outer nose radius	R_o	0.21 cm
Cavity inner corner radius	R_{ci}	0.50 cm
Septum thickness	s	1.00 cm
Drift-tube face angle	α_f	68 degrees
Drift-tube corner radius	R_c	0.50 cm
Drift-tube inner nose radius	R_{di}	0.07 cm
Drift-tube outer nose radius	R_{do}	0.21 cm
Drift-tube stem diameter	d_{stem}	1.016 cm
Number of stems per drift tube	N_{stem}	2
Ring inner radius	$R_{Ring,i}$	0.25 cm
Ring outer radius	$R_{Ring,o}$	0.25 cm

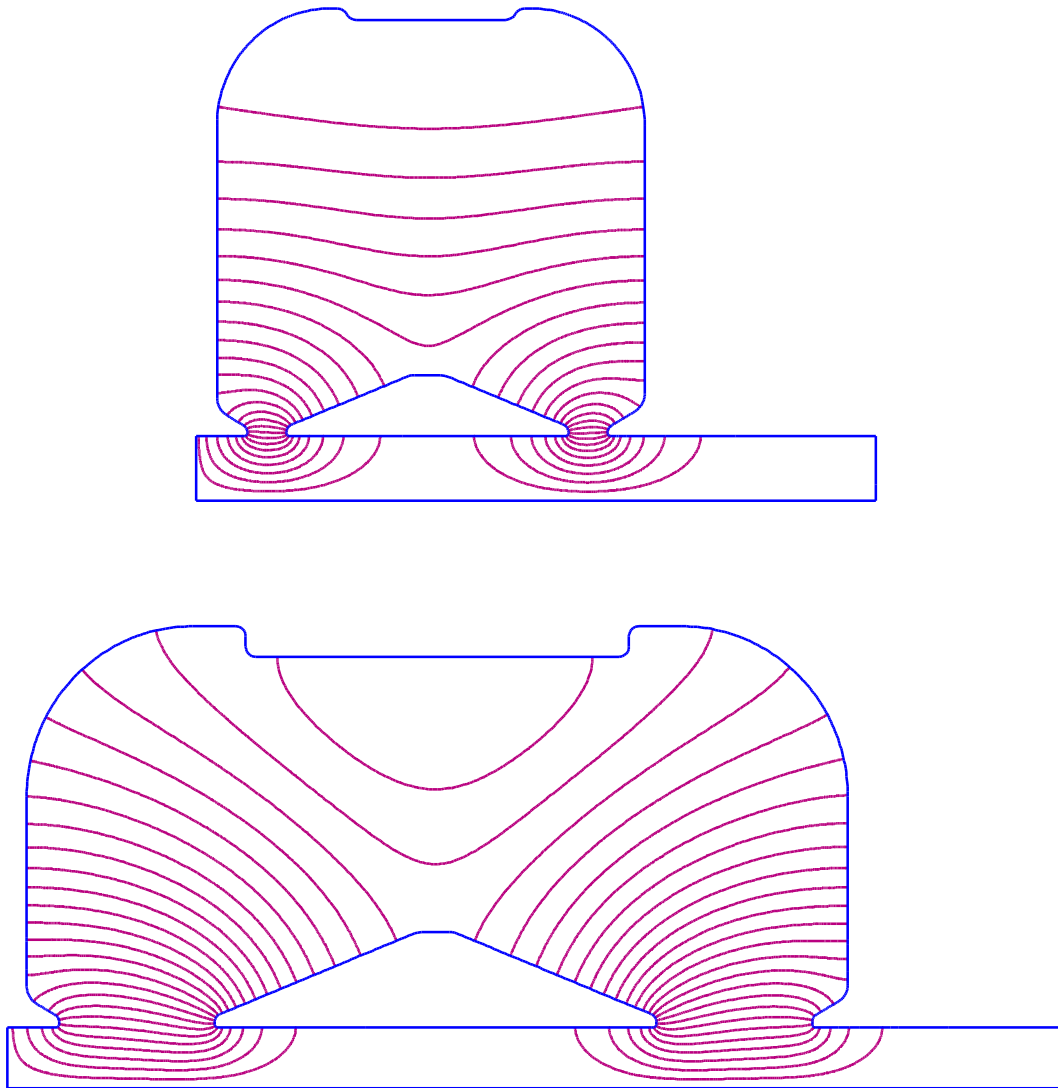


Figure 5. SUPERFISH generated cavity shapes for $b = 0.20$ (top) and $b = 0.39$ (bottom). Each contour line corresponds to a constant magnetic field H_f . The electric field is parallel to these contours.

Table 2. CCDTL Geometric Parameters that Vary with Particle Velocity.

β	g	$g/\beta\lambda$	Δg_1	Δg_2	d	F, F_d	F_{Eq}	R_{co}	W_{Ring}	D_{Ring}
0.20	0.92376	0.12402	-0.17578	0.01333	5.8	0.00	4.8	2.686	4.0	0.275
0.21	1.02326	0.13084	-0.16172	0.01510	5.9	0.00	5.2	2.766	4.3	0.300
0.22	1.12891	0.13779	-0.15100	0.01762	6.0	0.00	5.6	2.845	4.6	0.325
0.23	1.26611	0.14781	-0.14406	0.02083	6.1	0.02	6.0	2.924	4.9	0.350
0.24	1.40855	0.15759	-0.13954	0.02482	6.2	0.04	6.4	3.003	5.2	0.375
0.25	1.55616	0.16714	-0.13716	0.02978	6.3	0.06	6.8	3.083	5.5	0.400
0.26	1.68349	0.17387	-0.13553	0.03496	6.4	0.06	7.2	3.162	5.8	0.425
0.27	1.81597	0.18060	-0.13589	0.04122	6.5	0.06	7.6	3.241	6.1	0.450
0.28	1.95314	0.18731	-0.13803	0.04850	6.6	0.06	8.0	3.321	6.4	0.475
0.29	2.09594	0.19407	-0.14227	0.05678	6.7	0.06	8.4	3.400	6.7	0.500
0.30	2.24431	0.20088	-0.14841	0.06633	6.8	0.06	8.8	3.479	7.0	0.525
0.31	2.39842	0.20775	-0.15668	0.07726	6.9	0.06	9.2	3.559	7.3	0.550
0.32	2.55863	0.21470	-0.16723	0.08977	7.0	0.06	9.6	3.638	7.6	0.575
0.33	2.72578	0.22180	-0.18053	0.10414	7.1	0.06	10.0	3.717	7.9	0.600
0.34	2.90024	0.22905	-0.19637	0.12065	7.2	0.06	10.4	3.797	8.2	0.625
0.35	3.08605	0.23676	-0.21615	0.13998	7.3	0.06	10.8	3.876	8.5	0.650
0.36	3.27946	0.24461	-0.23984	0.16246	7.4	0.06	11.2	3.955	8.8	0.675
0.37	3.48440	0.25287	-0.26837	0.18798	7.5	0.06	11.6	4.034	9.1	0.700
0.38	3.70221	0.26161	-0.30319	0.21874	7.6	0.06	12.0	4.114	9.4	0.725
0.39	3.94013	0.27128	-0.34609	0.25522	7.7	0.06	12.4	4.193	9.7	0.750

From the output of the PARMILA program, we will obtain the cavity length (and hence geometric β) for each segment of the SNS linac. Then, with one exception, we linearly interpolate each parameter in Table 2. The exception is the initial depth of the tuning ring D_{Ring} , which will be a few millimeters larger in order to compensate for the frequency tuning effects of coupling slots and drift-tube stems. In Table 3, we estimate the additional depth required for the $\beta = 0.20$ and $\beta = 0.39$ cavities. The initial ring depth needs to be slightly larger than the expected depth after tuning. Calculation of the frequency effects of the slots assumed 5% coupling, and particular coupling cavities at each particle velocity. The coupling cavity diameter was 17.45 cm. The coupling cavity length was 5.31 cm for the $\beta = 0.20$ accelerating cavity and 6.74 cm for the $\beta = 0.39$ accelerating cavity.

All of the frequency tuning of the CCDTL cavities may be accomplished by modifying these tuning rings. We build the cavities with a deeper ring than we expect to have after tuning. Thus, the cavities are initially slightly high in frequency. During the low-power tuning procedure, we might remove too much material from the tuning ring. If we provide one or more thin regions on the outer surface of the tuning rings, then “dinging” the outer wall can make small increases in the cavity frequency.

Table 3. Estimate of the Initial Tuning Ring Depth.

Parameter	$\beta = 0.20$	$\beta = 0.39$
Ring depth for 805 MHz (no stems or slots)	0.265 cm	0.750 cm
Resonant frequency with ring removed	799.912 MHz	785.304 MHz
Tuning rate with ring depth	19.20 MHz/cm	26.26 MHz/cm
Frequency effect of both stems	+2.667 MHz	+2.091 MHz
Frequency effect of both coupling slots	-10.094 MHz	-7.392 MHz
Net frequency correction	-7.427 MHz	-5.301 MHz
Additional ring depth required	0.387 cm	0.202 cm
Expected ring depth after tuning	0.652 cm	0.952 cm
Initial ring depth	0.750 cm	1.000 cm

Table 4. CCDTL RF Parameters.

β	Q	ZT^2 (M Ω /m)	T	E_0T (MV/m)	E_p/E_K	U (J)	P (kW)
0.20	17,607	21.542	0.70558	1.92	1.32	0.0666	19.12
0.21	18,122	23.504	0.72078	2.05	1.35	0.0752	20.98
0.22	18,622	25.343	0.73383	2.20	1.38	0.0864	23.47
0.23	19,090	26.898	0.74453	2.36	1.35	0.1004	26.60
0.24	19,528	28.290	0.75361	2.50	1.34	0.1144	29.62
0.25	20,881	30.924	0.76124	2.64	1.34	0.1299	31.48
0.26	21,293	32.258	0.76860	2.75	1.37	0.1433	34.05
0.27	21,662	33.423	0.77488	2.87	1.40	0.1592	37.17
0.28	22,006	34.444	0.78016	2.98	1.44	0.1755	40.33
0.29	22,327	35.324	0.78445	3.02	1.43	0.1846	41.83
0.30	22,628	36.068	0.78788	3.04	1.43	0.1921	42.94
0.31	22,908	36.678	0.79052	3.05	1.42	0.1989	43.92
0.32	23,169	37.156	0.79238	3.06	1.42	0.2064	45.05
0.33	23,412	37.506	0.79348	3.07	1.41	0.2144	46.32
0.34	23,637	37.727	0.79390	3.07	1.44	0.2217	47.45
0.35	23,845	37.801	0.79350	3.08	1.41	0.2313	49.07
0.36	24,035	37.754	0.79244	3.08	1.41	0.2401	50.53
0.37	24,208	37.585	0.79072	3.08	1.42	0.2497	52.17
0.38	24,364	37.277	0.78824	3.09	1.43	0.2619	54.37
0.39	24,505	36.801	0.78485	3.09	1.44	0.2739	56.53

Shunt Impedance and Peak Surface Fields in the CCDTL

Table 4 contains a collection of some of the important rf parameters of the CCDTL. The cavity Q, shunt impedance ZT^2 , and the transit-time factor T are independent of field level. More detailed transit-time-factor integrals are available by electronic transfer as explained at the end of this memo. Data in the last three columns of Table 4 depend on the field level in the cavity and correspond to the design value of E_0T listed in column 5. The Q value, shunt impedance, and power include the power dissipated on stems and an estimate of the additional power dissipated near the coupling slots. For 5% cell-to-cell coupling in the CCDTL, the coupling slots in each cavity increases power dissipation by about 10%, which in turn reduces the Q and ZT^2 by 10%.

Figure 6 is a plot of shunt impedance versus β for the SNS CCDTL. The figure includes data from previous designs for comparison as well as a few points for the first section of CCL following the CCDTL. In the earlier memorandum on the CCDTL, AOT-1:TNM97-049, the shunt impedance plot did not include the additional power dissipated near the coupling slots. These data have been corrected for this comparison. The plot shows that the CCDTL is slightly more efficient than the CCL up to a particle velocity $\beta \sim 0.415$ (93 MeV). Nevertheless, the present design switches to a CCL at $\beta = 0.39$ (80 MeV) so that no rf module contains both type of cavities.

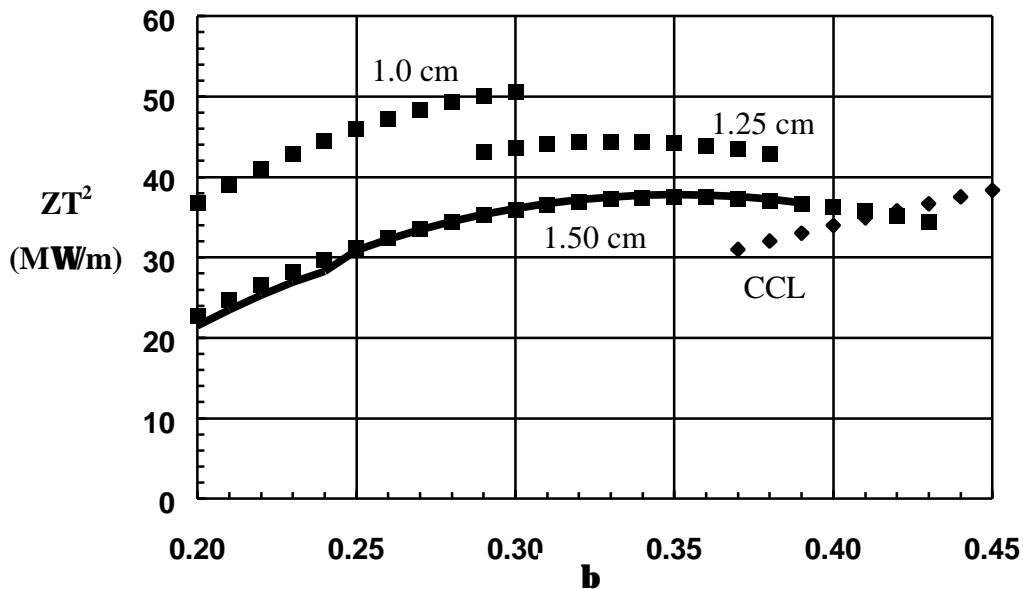


Figure 6. Effective shunt impedance ZT^2 versus particle velocity. The solid line is the present CCDTL redesign. Lengths in cm are bore radii. Square symbols are from previous CCDTL designs, and the diamond symbols are the first section of CCL, which also has a 1.5-cm bore radius.

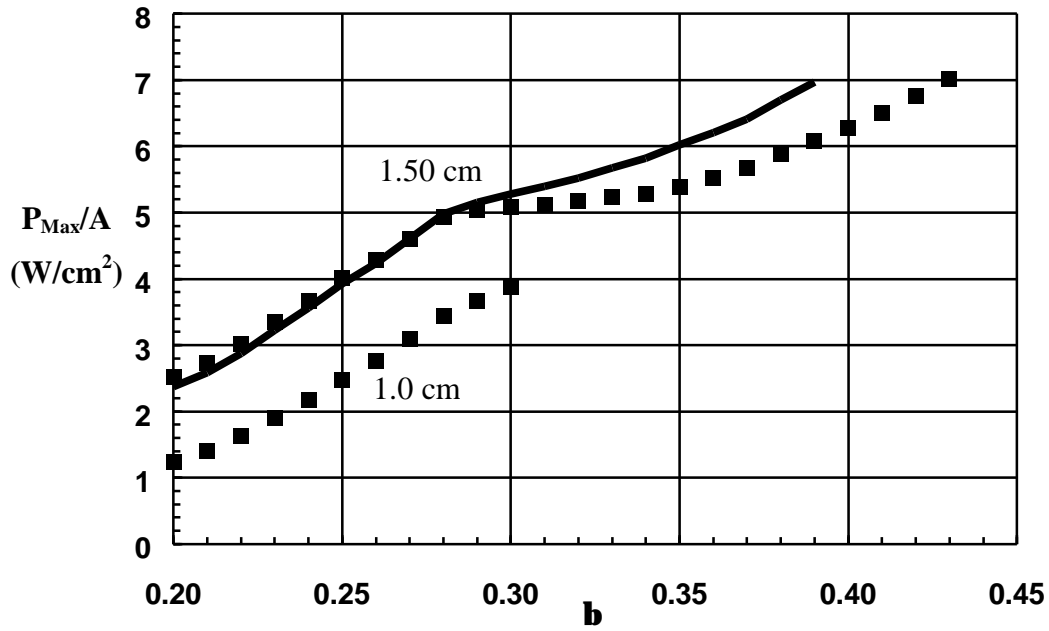


Figure 7. Peak power density versus particle velocity for the CCDTL. Lengths in cm are bore radii. The solid line is the present CCDTL redesign. Square symbols are from previous CCDTL designs.

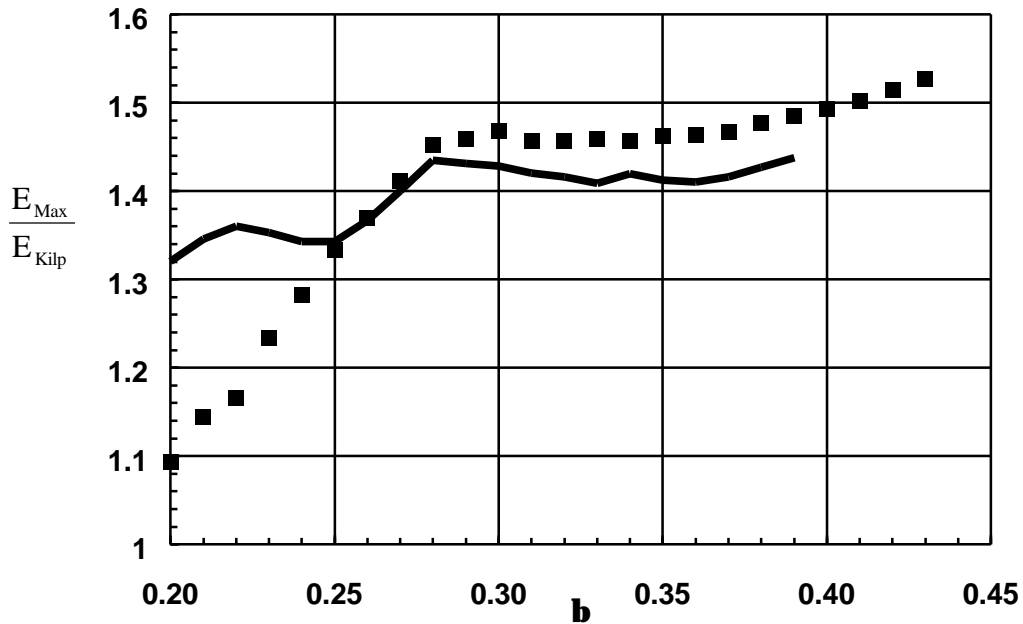


Figure 8. Peak surface electric field relative to the Kilpatrick field (26.0565 MV/m at 805 MHz) versus particle velocity. The solid line is the present CCDTL redesign. Square symbols are from a previous CCDTL design with 1.5-cm bore radius.

Figure 7 shows the peak power density in the SNS CCDTL computed by SUPERFISH for 6.76% rf duty factor at the accelerating fields E_0T listed in Table 4. This figure also includes data from previous designs. The location in the cavity of the peak power densities is the longitudinal center of the internal drift tube. Power densities on the cavity wall are typically only 20% to 50% of the maximum value that occurs on the drift tube. The drift-tube stems attach at the location of the maximum power density. This proximity of the stems results in an even higher local power density on the stems and on the drift-tube body because of the distortion of the magnetic field around the circular stems. The magnetic field around the circumference of a circular stem (that has been inserted into an otherwise uniform field distribution) has a sinusoidal pattern with a maximum value equal to twice the unperturbed cavity field. The peak power density at two points on the stem circumference is four times the power density that corresponds to the unperturbed fields. The integrated power density around the stem circumference is thus twice as high as the unperturbed value because the average of the sine-squared function is 0.5.

Figure 8 shows the peak surface electric field for the accelerating fields E_0T listed in Table 4. For the frequency of 805 MHz, Kilpatrick's criterion is equal to 26.0565 MV/m. These peak electric fields occur near the tip of the internal drift-tube noses. The electric field on the cavity wall noses is lower than that on the internal drift-tube noses. None of the cavities exceed 1.45 Kilpatrick at the present design field levels.

Data Files

The SUPERFISH input and output files for the CCDTL are available in the shared directory \\pc-billen\Projects\NSNS\CCDTL\N1.500. (If you are not a member of the AOT-1 computer domain, log in to machine pc-billen.atdiv.lanl.gov by FTP as user Linac with password aot1ftp.)

Electronic Distribution:

A. J. Jason, LANSCE-1, ajason@lanl.gov
F. L. Krawczyk, LANSCE-1, fkrawczyk@lanl.gov
S. S. Kurennoy, LANSCE-1, kurennoy@lanl.gov
T. S. Bhatia, LANSCE-1, tsb@lanl.gov
R. D. Ryne, LANSCE-1, ryne@lanl.gov
J. Qiang, LANSCE-1, jiqiang@lanl.gov
S. Nath, LANSCE-1, snath@lanl.gov
D. L. Schrage, LANSCE-1, dls@lanl.gov
J. D. Gilpatrick, LANSCE-1, gilpatrick@lanl.gov
R. Garnett, LANSCE-1, rgarnett@lanl.gov
J. E. Stovall, LANSCE-1, jstovall@lanl.gov
H. Takeda, LANSCE-1, htakeda@lanl.gov
T. P. Wangler, LANSCE-1, twangler@lanl.gov
M. T. Lynch, LANSCE-5, mtlynch@lanl.gov
P. J. Tallerico, LANSCE-5, tallerico@lanl.gov
N. K. Bultman, ESA-EA, nbultman@lanl.gov
P. Grand, TechSource, pgrand@ibm.net
B. K. Hartline, LANSCE-SNS, hartline@lanl.gov
R. A. Hardekopf, LANSCE-SNS, hardekopf@lanl.gov

Hard Copy Distribution:

S. O. Schriber, LANSCE-DO, H850
LANSCE-1 Reading File, H808
LANSCE-DO, H850
SNS Project Office, H824